9th IFAC Conference on Control Applications in Marine Systems
The International Federation of Automatic Control
September 17-20, 2013. Osaka, Japan

Modelling for Control of Exhaust Gas Recirculation on Large Diesel Engines

Jakob Mahler Hansen [*,**] **Claes-Göran Zander** [**]
Nicolai Pedersen [*] **Mogens Blanke** [*,***]
Morten Vejlgaard-Laursen [**]

[*] *Automation and Control Group, Dept. of Electrical Engineering, Technical University of Denmark, Kgs. Lyngby, Denmark*
[**] *MAN Diesel & Turbo, Copenhagen, Denmark*
[***] *AMOS Centre of Excellence, Norwegian University of Science and Technology, Trondheim, Norway*

Abstract: Exhaust Gas Recirculation (EGR) reduces NO_x emissions by reducing O_2 concentration for the combustion and is a preferred way to obtain emission regulations that will take effect from 2016. If not properly controlled, reduction of O_2 has adverse side effects and proper control requires proper dynamic models. While literature is rich on four-stroke automotive engines, this paper considers two-stroke engines and develops a non-linear dynamic model of the exhaust gas system. Parameters are determined by system identification. The paper uses black-box nonlinear model identification and modelling from first principles followed by parameter identification and compares the results of these approaches. The paper performs a validation against experimental data from a test engine and presents a linearised model for EGR control design.

Keywords: NOx emission; Exhaust gas recirculation; Diesel engine; Identification; Green Ship.

1. INTRODUCTION

With increasing environmental awareness, the International Maritime Organisation (IMO) has required limiting of emissions by marine diesel engines. The protocols concern emission of NO_x, SO_x and greenhouse gasses.

Exhaust Gas Recirculation (EGR) technology reuses the engine exhaust gas in the combustion in order to reduce the amount of oxygen in the engine intake and thereby reduce the amount of NO_x created by the combustion. There is, however, a limit to how much exhaust gas can be recirculated without reducing the air-to-fuel ratio below its lowest acceptable level where the engine is deprived of sufficient oxygen and harmful side effects will occur.

While significant EGR research has been devoted for truck engines Wahlström and Eriksson [2011a,b, 2008], Wahlström et al. [2010], van Nieuwstadt et al. [2000], little knowledge has been published on dynamic models of exhaust gas recirculation dynamics for large marine diesel engines, which differ significantly in their combustion and scavenging cycles from those of a truck engine. Modelling of the engine control properties has been dealt with and very good mean value models for control design were made available in the now classical literature, see Hendricks [1989], Blanke and Andersen [1984], but the engines of that time did not include exhaust gas recirculation.

This paper employs first a black-box structure of the air-path. Physical principles are then used to model the highly non-linear behaviours of components in the EGR loop, using related work for truck engines Wahlström and Eriksson [2011b], significant modifications are made to capture the particularities of the combustion cycle of large diesel engines. The parameters in the non-linear model are then identified from engine tests using dedicated signals for identification. Model quality are investigated after fitting of parameters using data-driven identification methods. The results are input to output transfer functions for control system analysis and design.

The paper first introduces the EGR loop components. A black-box model is then formulated and identification results are evaluated. Non-linear dynamics are then modelled from first principles using available non-linear characteristics of essential components. Results are validated by engine tests and conclusions summarise the paper.

2. EXHAUST GAS RECIRCULATION

The engine considered in this study is a two-stroke diesel 4T50ME-X engine with four cylinders, from MAN Diesel & Turbo. The air intake for the engine is supplied by a Variable Geometry Turbocharger (VGT), consisting of a common shaft compressor and turbine. Air pressures are measured at the scavenge and exhaust air manifolds.

The EGR-loop connects the two manifolds, where a blower provides a mass flow from exhaust to scavenge manifold. Exhaust gas passes through a scrubber, a cooling unit, a blower and a valve. We assume there is no effect on mass flow from neither the scrubber nor from two cooling units that decrease gas temperature. The blower avoids backflow in the EGR-loop.

Input signals are valve opening, u_{egr}, and blower speed, ω_{blow}. Disturbance signals in this context are VGT opening, u_{vgt} and engine load, u_{load}. The latter is relative power

delivered to the shaft. It is desired to control the scavenge oxygen concentration, O_{scav}, which is the output of the model.

Fig. 1 illustrates the gas recirculation where the inputs and disturbances are marked with arrows. Signals measured on the 4T50ME-X test engine are underlined.

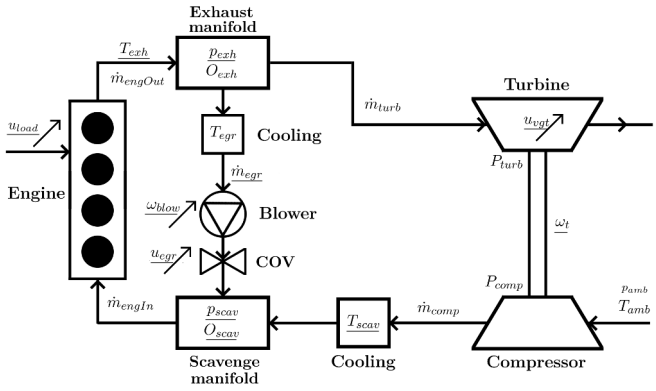

Fig. 1. Model structure of the engine system. There are two control inputs (u_{egr} and ω_{blow}) and two disturbance inputs (u_{vgt} and u_{load})

3. NON-LINEAR BLACK-BOX MODELLING

Due to the complexity and strong non-linearity of the engine air-path physics, a black-box model is first identified. A non-linear autoregressive model with exogenous input (NARX) is chosen as black-box model and a wavelet network is used as non-linear estimator.

3.1 Non-linear autoregressive model with exogenous input

The autoregressive model with exogenous input (ARX) has been used to estimate similar physical systems eg. Cajueiro et al. [2012]; Sjoeberg et al. [1995] and more,

$$\begin{aligned} &y(t) + a_1 y(t-1) + .. + a_{n_a} y(t-n_a) = \\ &b_1 u(t-n_k) + .. + b_{n_b} u(t-(n_k+n_b+1)). \end{aligned} \tag{1}$$

Here n_k is delay from input to output, n_a the number of past output terms used and n_b the number of past input terms. By isolating $y(t)$ in Eq. 1 the one step ahead prediction is determined as the weighted sum of past observations. This is formulated by a regression vector $\varphi(t)$ and a coefficient vector θ,

$$\begin{aligned} y(t) =&[-a_1, .. - a_{n_a}, b_1, .., b_{n_b}][y(t-1), .., y(t-n_a), \\ &u(t-n_k), .., u(t-(n_k+n_b+1))]^T = \theta\varphi^T(t). \end{aligned} \tag{2}$$

For non-linear ARX (NARX) models, a non-linear mapping $g()$ between input and output is furthermore used, and the NARX structure can be a series-parallel combination of regressors subject to replicate both a linear and non-linear relations,

$$y(t) = g(\varphi(t)) + \varphi(t)\theta^T + y_0, \tag{3}$$

where y_0 is a scalar output offset.

3.2 Wavelet network

As non-linear mapping, $g(\varphi)$ from Eq. 3, a wavelet network was found beneficial by Sjoeberg et al. [1995], Zhang and Benveniste [1992]. The *wavenet* they introduced is a wavelet decomposition implemented as a one hidden-layer neural network:

$$g(\varphi) = \sum_{i=1}^{N} w_i \psi[D_i(\varphi - t_i)], \tag{4}$$

where $\psi()$ is the mother wavelet, w_i is a weighing factor, D_i is a dilation and t_i is a translation.

A model was created using measured data from the MAN test-engine. The input signals (u_{egr} and ω_{blow}) together with the disturbances (u_{vgt} and u_{load}) were used as model input and O_{scav} the output. Regressor orders $n_a = 3$, $n_b = 3$ with a single wavenet unit resulted in a 82% fit to the training data shown in Fig. 2.

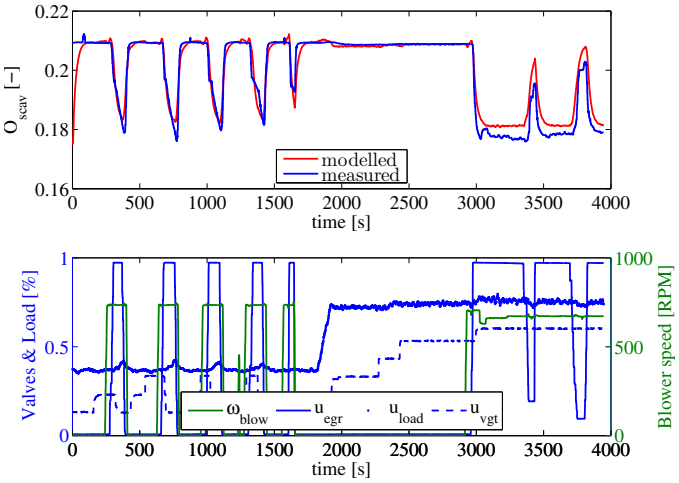

Fig. 2. Comparison of measurement and black-box estimation for the training dataset. Fit is 82% on O_{scav}.

However, when applying actuator data from different tests, the model fit declines dramatically. Fig. 3 shows such a case where the model fit is only 20 %. We therefore conclude that the NARX black-box modelling is too sensitive to the exact input sequence on training data and that some over-parametrisation can easily occur when practical tests do not provide sufficiently rich excitation. The effort was therefore turned towards physical modelling to allow grey-box identification of parameters in a non-linear model with a physical structure derived from first principles.

4. NON-LINEAR STATE SPACE MODEL

A non-linear state space model can be made from first physical principles as was shown for a four-stroke diesel truck in eg. Wahlström and Eriksson [2011b]. The large two-stroke engines are quite different in their scavenging cycle, so an independent modelling effort is needed. The model will be shown to consist of seven differential equations and two difference equations. The nine states are listed in Table A.1. The two discrete states relate to exhaust gas temperature, see Sec. 4.3.3.

4.1 Compressor

The mass flow through the compressor is determined using a compressor map. The map describes the compressor

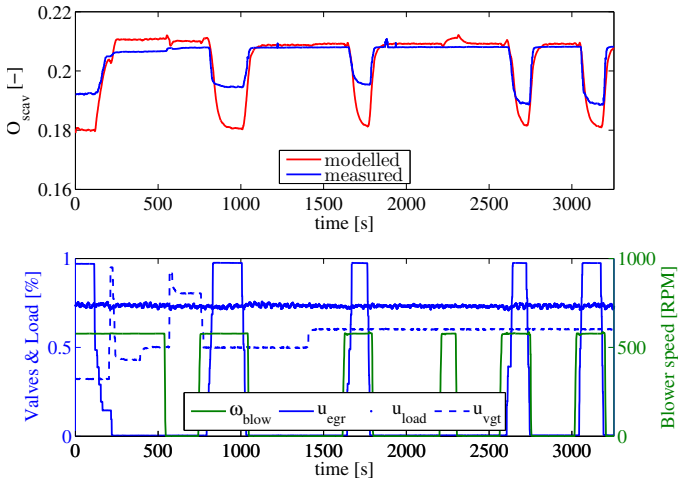

Fig. 3. Comparison of engine measurement and black-box estimation for a verification dataset. Fit is only 20% on O_{scav}.

mass flow from the pressure ratio and the speed of the turbocharger.

The polynomial describing the mass flow is a two dimensional forth order polynomial of the pressure ratio $\Pi_c = [p_{scav}/p_{amb}]$ and turbocharger speed, ω_t,

$$\dot{m}_{comp} = \sum_{n=0}^{4}\sum_{m=0}^{4} C_{mass}(n,m)\omega_t^n \Pi_c^m, \tag{5}$$

where $C_{mass}(n,m)$ is a vector of 25 compressor mass flow coefficients found using SENSTOOLS, Knudsen.

The power required to run the compressor is formulated as, Jankovic et al. [2000], Wahlström and Eriksson [2011b],

$$P_{comp} = \frac{\dot{m}_{comp} c_{pa} T_{amb}}{\eta_c}\left(\Pi_c^{1-1/\kappa_a} - 1\right), \tag{6}$$

where the compressor efficiency, η_c can be found from the compressor map. The efficiency is estimated as,

$$\eta_c = \sum_{n=0}^{4}\sum_{m=0}^{4} C_{\eta}(n,m)\omega_t^n \Pi_c^m, \tag{7}$$

where $C_\eta(n,m)$ is a vector of 25 compressor efficiency coefficients.

4.2 Manifolds

In the scavenge manifold gas-flows from the compressor and EGR-loop are mixed and sent to the engine intake. The exhaust manifold splits the exhaust gas into two mass flows; through the turbine and through the EGR-loop.

Pressure The pressure is a function of the difference in the incoming and outgoing mass flows, and can be described as, see Abidi et al. [2012], Dabo et al. [2008], Jankovic et al. [2000], Wahlström et al. [2010], Wahlström and Eriksson [2008, 2011a,b],

$$\frac{d}{dt}p_{scav} = \frac{R_a}{V_{scav}}(T_{scav}\dot{m}_{comp} + T_{egr}\dot{m}_{egr} - T_{scav}\dot{m}_{engIn}) \tag{8}$$

$$\frac{d}{dt}p_{exh} = \frac{R_e T_{exh}}{V_{exh}}(\dot{m}_{engOut} - \dot{m}_{turb} - \dot{m}_{egr}), \tag{9}$$

where V_{scav} and V_{exh} are the constant volumes.

Oxygen concentration The oxygen concentration is measured as a volume percentage, where maximum is 20.95% of the air, corresponding to the ambient oxygen-to-air ratio. The minimum allowed concentration of oxygen is determined by the engine. If the concentration is too low, the engine will produce black smoke and might be damaged. The concentration is modelled using a first order differential equation, Wahlström et al. [2010], Wahlström and Eriksson [2008, 2011a,b],

$$\frac{d}{dt}O_{scav} = \frac{R_a}{p_{scav}V_{scav}}((O_{exh} - O_{scav})T_{egr}\dot{m}_{egr} + (O_{comp} - O_{scav})T_{scav}\dot{m}_{comp}) \tag{10}$$

$$\frac{d}{dt}O_{exh} = \frac{R_e T_{exh}}{p_{exh}V_{exh}}(O_{eng} - O_{exh})\dot{m}_{engOut}, \tag{11}$$

where O_{scav}, O_{exh} and O_{comp} are the oxygen ratios in the scavenge manifold, exhaust manifold and compressor air, respectively. The temperatures, T_{egr} and T_{scav}, have been assumed constant. R_a and R_e are the specific ideal gas constant for fresh air and exhaust gas, respectively.

4.3 Engine

When passing through the engine the temperature of the mass flow will increase and part of the oxygen in the intake will be used in the creation of NO_x, CO_2 and H_2O.

Mass flows The mass flows through the engine is modelled as flow through a restriction, as in Egeland and Gravdahl [2003], Theotokatos [2010],

$$\dot{m}_{engIn} = \frac{A_{eng}p_{scav}}{\sqrt{R_a T_{scav}}}\sqrt{\frac{2\kappa_a}{\kappa_a - 1}\left(\Pi_{eng}^{2/\kappa_a} - \Pi_{eng}^{1+1/\kappa_a}\right)}, \tag{12}$$

where $\Pi_{eng} = [p_{exh}/p_{scav}]$ is the pressure ratio over the engine, and A_{eng} is the cross sectional area of the engine inlet.
During the combustion fuel is added and the mass flow out of the engine is therefore,

$$\dot{m}_{engOut} = \dot{m}_{engIn} + \dot{m}_{fuel}. \tag{13}$$

The engine load is proportional to the fuel mass flow $\dot{m}_{fuel}$ which can be found as a constant gain to the measured engine load,

$$\dot{m}_{fuel} = u_{load}\ k_{loadToFuel}. \tag{14}$$

Oxygen The oxygen concentration is determined using the equations suggested by Wahlström and Eriksson [2008, 2011a,b],

$$O_{eng} = \frac{\dot{m}_{engIn}O_{scav} - \dot{m}_{fuel}OF_s O_{comp}}{\dot{m}_{engOut}}, \tag{15}$$

where the second term in the numerator is the amount of reacting oxygen. The constant OF_s describes the stoichiometric ratio of oxygen mass to fuel mass.

Temperature The calculation of exhaust gas temperature is a cyclic process which depends on the pressure ratio, fuel injection and mass flow intake. Equations for the estimation of the exhaust gas temperature are found in Wahlström and Eriksson [2011b] and repeated here,

$$T_{exh,k+1} = \eta_{sc}\Pi_{eng}^{1-1/\kappa_a} r_c^{1-\kappa_a} x_{p,k+1}^{1/\kappa_a - 1}(q_{in,k+1} \cdot \left(\frac{1-x_{cv}}{c_{pa}} + \frac{x_{cv}}{c_{va}}\right) + T_{1,k} r_c^{\kappa_a - 1}), \tag{16}$$

where $\Pi_{eng} = \frac{p_{exh}}{p_{scav}}$ is the pressure ratio over the engine, η_{sc} is a compensation factor due to the non-ideality of the combustion cycles. The constants r_c and x_{cv} are the compression ratio and the ratio of fuel burned at constant volume combustion, respectively.
The expressions for the variables in Eq. 16 are given by, Wahlström and Eriksson [2011b],

$$x_{p,k+1} = 1 + \frac{q_{in,k+1} x_{cv}}{c_{va} T_{1,k} r_c^{\kappa_a - 1}} \tag{17}$$

$$q_{in,k+1} = \frac{\dot{m}_{fuel} LHV}{\dot{m}_{engIn} + \dot{m}_{fuel}} (1 - x_{r,k}) \tag{18}$$

$$x_{r,k+1} = \frac{\Pi_{eng}^{1/\kappa_a} x_{p,k+1}^{-1/\kappa_a}}{r_c x_{v,k+1}} \tag{19}$$

$$x_{v,k+1} = 1 + \frac{q_{in,k+1} (1 - x_{cv})}{c_{pa} \left(\frac{q_{in,k+1} x_{cv}}{c_{va}} + T_{1,k} r_c^{\kappa_a - 1} \right)} \tag{20}$$

$$T_{1,k+1} = x_{r,k+1} T_{exh,k+1} + (1 - x_{r,k+1}) T_{scav}, \tag{21}$$

where x_p is the pressure ratio between before and after the combustion, q_{in} is the specific energy contents of the mixed mass flows, x_r is the gas fraction of the remaining gas, x_v is the volume ratio between after and before the combustion, and T_1 is the temperature after the intake stroke.

4.4 Turbine

The turbine is equipped with a variable opening, making it possible to get higher shaft speeds with less mass flow. The higher the exhaust gas mass flow, the faster the shaft rotates.

VGT-signal The measurements indicate that the VGT actuator signal should be modelled as,

$$\hat{u}_{vgt} = \frac{1}{\tau_{vgt} s + 1} u_{vgt}, \tag{22}$$

with time constant τ_{vgt}.

Mass flow The mass flow through the turbine is described in the turbine maps. The map data describes the normalised mass flow through the turbine as a function of the pressure ratio over the turbine, the turbocharger speed and the opening of the VGT vanes. The mass flow has been normalised with the pressure and temperature in the exhaust manifold using SAE standards,

$$k_{vgt}(\hat{u}_{vgt}) = a \hat{u}_{vgt}^2 + b \hat{u}_{vgt} + c \tag{23}$$

$$f_{turb}(\Pi_t, \omega_t) = \sum_{n=0}^{4} \sum_{m=0}^{4} T_{mass}(n,m) \omega_t^n \Pi_t^m \tag{24}$$

$$\dot{m}_{turb,norm} = k_{vgt}(\hat{u}_{vgt}) f_{turb}(\Pi_t, \omega_t). \tag{25}$$

The coefficients for the polynomial vector $T_{mass}(n,m)$ are found using a least squares fit.

The equation describing the mass flow, is normalised and can be converted by,

$$\dot{m}_{turb}[kg/s] = \frac{\dot{m}_{turb,norm} \left[\frac{(kg\sqrt{K})}{(s \cdot kPa)} \right] p_{exh}[kPa]}{\sqrt{T_{exh}[K]}}, \tag{26}$$

where the units of the parameters are included to emphasise that the pressure is in $[kPa]$.

Speed The speed of the turbocharger shaft is determined by the power required of the compressor and the power supplied by the turbine. The speed is calculated as, Dabo et al. [2008], Jankovic et al. [2000], Wahlström et al. [2010], Wahlström and Eriksson [2011b],

$$\frac{d}{dt}\omega_t = \frac{P_t \eta_m - P_{comp}}{J_t \omega_t}, \tag{27}$$

where P_t is the power supplied by the turbine, P_{comp} is the power required by the compressor and J_t is the moment of inertia of the shaft.

The power created by the turbine is determined as, Abidi et al. [2012], Jankovic et al. [2000], Wahlström and Eriksson [2011b],

$$P_t \eta_m = \eta_t \dot{m}_{turb} c_{pe} T_{exh} \left(1 - \left(\frac{p_{amb}}{p_{exh}} \right)^{1 - 1/\kappa_e} \right), \tag{28}$$

where the constant c_{pe} is the specific heat capacity for exhaust gas at constant pressure.

Efficiency The turbine efficiency η_t is the most complex part of the maps and is highly dependent of both the pressure ratio over the turbine, the turbocharger speed and the opening of the VGT vanes. The efficiency is modelled as,

$$\eta_t = v_{turb}(h_{turb}(\Pi_t, \omega_t), u_{vgt}) \tag{29}$$

Where h_{turb} and $v_{turb}(h_{turb}, U_{vgt})$ are two dimensional fourth order polynomials,

$$h_{turb}(\Pi_t, \omega_t) = \sum_{n=0}^{4} \sum_{m=0}^{4} T_h(n,m) \omega_t^n \Pi_c^m \tag{30}$$

and

$$v_{turb}(h_{turb}, u_{vgt}) = \sum_{n=0}^{4} \sum_{m=0}^{4} T_v(n,m) h_{turb}^n u_{vgt}^m, \tag{31}$$

where $T_h(n,m)$ and $T_v(n,m)$ are vectors containing the polynomial coefficients.

4.5 EGR

The purpose of the blower in the EGR-loop is to ensure that the gas can flow despite the increase in pressure from exhaust to scavenge manifold. The Change-Over-Valve (COV) controls the amount of gas being recirculated. The mass flow through the EGR-loop is affected by two control signals; u_{egr} and ω_{blow}.

The mass flow is modelled as a compressor followed by a flow restriction. The mass flow leaving the EGR-loop from the valve is,

$$\dot{m}_{egr} = \frac{u_{egr} A_{egrmax} p_{blow}}{\sqrt{R_e T_{scav}}} \sqrt{\frac{2\kappa_e}{\kappa_e - 1} \left[\frac{p_{scav}}{p_{blow}}^{\frac{2}{\kappa_e}} - \frac{p_{scav}}{p_{blow}}^{\frac{\kappa_e + 1}{\kappa_e}} \right]}, \tag{32}$$

where A_{egrmax} is the maximum orifice of the COV and p_{blow} is the pressure at the valve inlet. p_{blow} can be calculated as a balance equation comparing the mass flow from the blower $\dot{m}_{blow}$ with the flow leaving the valve $\dot{m}_{egr}$ Egeland and Gravdahl [2003],

$$\frac{d}{dt} p_{blow} = \frac{c_p^2}{V_p} (\dot{m}_{blow} - \dot{m}_{egr}). \tag{33}$$

Here c_p is the sonic velocity $\sqrt{\kappa_e R_e T_{scav}}$ and V_p is the volume of the plenum between the blower and valve.

The mass flow from the blower $\dot{m}_{blow}$ is modelled as a compressor with velocity ω_{blow}, see Wahlström and Eriksson [2011b],

$$\dot{m}_{blow} = \frac{p_{exh}\pi R_{blow}^3 \omega_{blow} \Phi_{blow}}{R_e T_{egr}}. \quad (34)$$

The parameter Φ_{blow} has been altered from the suggestions in Wahlström and Eriksson [2011b], to allow for linearisation, without changing the functionality,

$$\Gamma_{blow} = \frac{1 - c_{\Psi 1}\Psi_{blow}^2}{c_{\Phi 1}} \quad (35)$$

$$\Phi_{blow} = \sqrt{\sqrt{\Gamma_{blow}^2}\frac{1}{2}\left(\frac{\Gamma_{blow}}{\sqrt{\Gamma_{blow}^2}} + 1\right)} \quad (36)$$

$$\Psi_{blow} = \frac{2c_{pe}T_{egr}}{R_{blow}^2\omega_{blow}^2}\left(\left(\frac{p_{blow}}{p_{exh}}\right)^{1-1/\kappa_e} - 1\right) \quad (37)$$

$$c_{\Psi 1} = c_{\omega\Psi blow}\begin{bmatrix}\omega_{blow}^2 & \omega_{blow} & 1\end{bmatrix}^T \quad (38)$$

$$c_{\Phi 1} = c_{\omega\Phi blow}\begin{bmatrix}\omega_{blow}^2 & \omega_{blow} & 1\end{bmatrix}^T. \quad (39)$$

4.6 Model fit

The response of the non-linear model has been compared to the measured signals from the 4T50ME-X diesel engine. Fig. 4 shows the oxygen concentration for the two datasets.

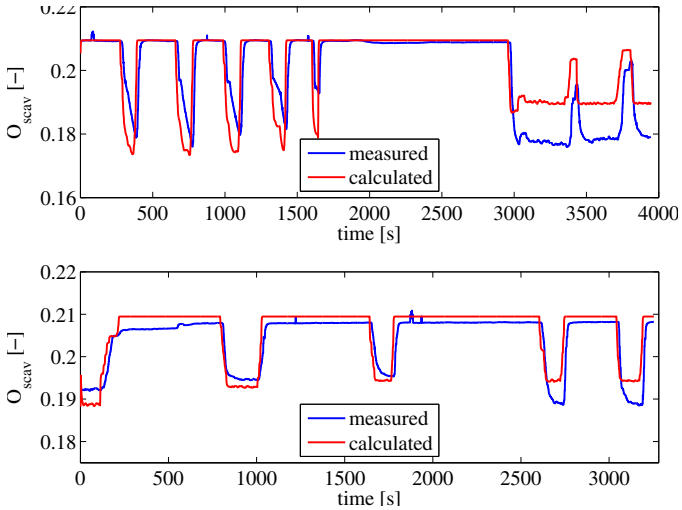

Fig. 4. Comparison of the measured and modelled oxygen concentration in the scavenge manifold. Top: estimation dataset, bottom: validation dataset

The model fits the measurement well for engine loads around 35%, which is the lowest engine load for the system configuration. An offset has been observed at engine loads of 75%, however, it is assumed that a better fit can be obtained for this region with more data available. A delay in the measurement of the oxygen is also detected. In the validation dataset the model has an offset when the COV is closed, also for the last two EGR steps the model reacts similar as the two previous which is expected from the input data, but does not match the measured signal. This indicates that some dynamics might be missing, e.g. the EGR blower diffuser or cooling effect, which would have to be considered for an improved model.

4.7 Linear Transfer Function Model for Control Design

The non-linear model is linearised around an operation point for 35% engine load. The linear model is represented on transfer function form, describing the transition from inputs and disturbances to the output, see Fig. 5

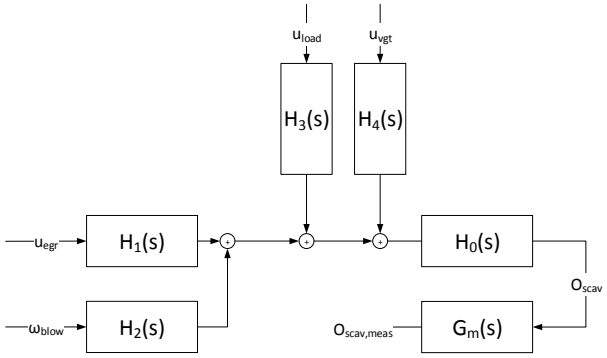

Fig. 5. Transfer function model with two control inputs (u_{egr} and ω_{blow}), two disturbance inputs (u_{vgt} and u_{load}) and a measurement delay $G_m(s)$

The model experiences a measurement delay denoted $\boldsymbol{G}_m(s) = e^{-\tau_d s}$.

To simplify the model the VGT disturbance is ignored and only the engine load $d = u_{load}$ is considered. The simplified model with three transfer functions is given as,

$$\boldsymbol{G}_{egr} \triangleq \boldsymbol{H}_1\boldsymbol{H}_0 = \frac{-3.25(s+3.53)(s^2+0.59s+0.13)}{(s+9.92)(s+1.56)(s+0.48)(s+0.19)}, \quad (40)$$

$$\boldsymbol{G}_{blow} \triangleq \boldsymbol{H}_2\boldsymbol{H}_0 = \frac{-11.47(s^2+0.59s+0.13)}{(s+9.92)(s+1.56)(s+0.48)(s+0.19)}, \quad (41)$$

$$\boldsymbol{G}_{d} \triangleq \boldsymbol{H}_3\boldsymbol{H}_0 = \frac{-0.78(s+11.54)(s+0.16)}{(s+9.92)(s+1.56)(s+0.48)(s+0.19)}. \quad (42)$$

The transfer functions are depicted in the Bode plot in Fig. 6 along with the approximate frequency interval of sea-waves. As the waves impact the propeller load and the engine's shaft speed control (governor) will react to this through corrective adjustments to the fuel flow, thus so will the engine load and the disturbance d will fluctuate at wave frequencies. Similarly disturbances will be created by manoeuvring activity and rudder commands below the wave range, caused by un-symmetric wake and other phenomena. Fig. 6 shows that $|\boldsymbol{G}_{egr}(j\omega)| < |\boldsymbol{G}_d(j\omega)|$ and $|\boldsymbol{G}_{blow}(j\omega)| < |\boldsymbol{G}_d(j\omega)|$ in parts of this frequency region, which is a challenge to EGR control. The control applications of the model are investigated in a companion paper Hansen et al. [2013].

5. CONCLUSION AND FUTURE DIRECTIONS

The paper presented modelling of a two-stroke low-speed diesel engine to allow control of the scavenge-air oxygen

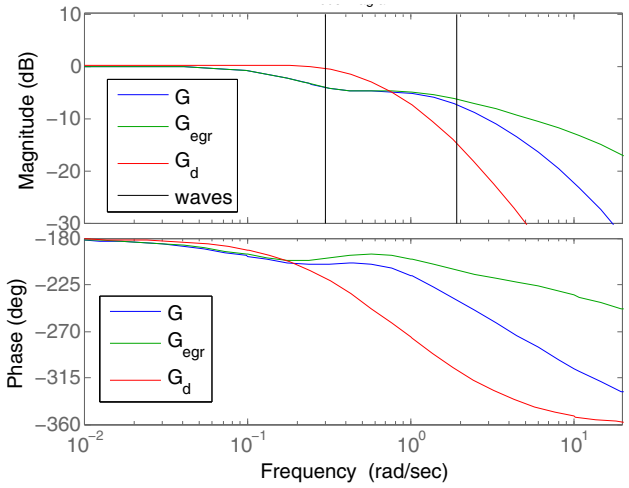

Fig. 6. Bode plot of $\boldsymbol{G}(s)$ and $\boldsymbol{G}_d(s)$ from the physical model and the wave frequency interval indicated with black vertical lines

concentration and thereby enable NO_x reduction. A non-linear black-box model fell short on validation data. A physical model with 9 states gave fine results for engine loads around 35 % and 50 % but showed an offset at 75 %. A linearised model was offered for 35% load. The control properties are analysed in a companion paper. Issues that were outside the scope of this paper, include identifiability and design of suitable input excitations. Cooler effects and pressure dependency of the time-delay in the O_{scav} measurement will be worthwhile to study further.

REFERENCES

I. Abidi, J. Bosche, A. Ei Hajjaji, and A. Aitouche. Control of a turbocharged diesel engine with egr system using takagi-sugenos approach. *20th Medit. Conf. Control & Automation (MED)*, -:960–9665, 2012.

M. Blanke and J. S. Andersen. On modelling large two stroke diesel engines: New results from identification. In *Proc. 9th Triennial IFAC World Congress, Hungary*, volume -, pages 2015–2020, 1984.

E. Cajueiro, R. Kalid, and L. Schnitman. Using narx model with wavelet network to inferring the polished rod position. *Mathematics and Computers in Simulation*, 6: 66–73, 2012.

M. Dabo, N. Langlois, W. Respondek, and H. Chafouk. Ncgpc with dynamic extension applied to a turbocharged diesel engine. In *Proc. 17th World Cong. The Inter. Fed. of Automatic Control Seoul, Korea, 2008*, pages 12065 –12070, July 2008.

O. Egeland and T. Gravdahl. *Modeling and Simulation for Automatic Control*. Marine Cybernetics, 2003.

J. M. Hansen, M. Blanke, H. H. Niemann, and M. Vejlgaard-Laursen. Exhaust gas recirculation control for large diesel engines - achievable performance with siso design. *IFAC, 9th Conference on Control Application in Marine Systems*, -:–, 2013.

E. Hendricks. Mean value modelling of large turbocharged two-stroke diesel engines. *SAE Technical paper series, 890564*, pages 1–13, 1989.

M. Jankovic, M. Jankovic, and I. Kolmanovsky. Constructive lyapunov control design for turbocharged diesel engines. *IEEE Trans. Control Systems Technology*, 8 (2):288–299, 2000.

M. Knudsen. Senstools. `http://www.control.auc.dk/~mk/ExpMod/SENSTOOLS/`, -.

J. Sjoeberg, Q. Zhang, L. Ljung, A. Benveniste, B. Delyon, P. Y. Glorennec, H. Hjalmarsson, and A. Juditsky. Nonlinear black-box modeling in system identification: a unified overview. *Automatica Oxford*, 31(12):1691–1724, 1995. ISSN 0005-1098.

G. Theotokatos. On the cycle mean value modelling of a large two-stroke marine diesel engine. *Proc. Inst. Mech. Eng., Part M: J. Eng. Marit. Environ.*, Vol. 224, no. 3: 193–205, 2010.

M. J. van Nieuwstadt, I. V. Kolmanovsky, P. E. Moraal, A. Stefanopoulou, and M. Jankovic. Egr-vgt control schemes: experimental comparison for a high-speed diesel engine. *IEEE Tr. Control Syst. Technology*, 20: 63–79, 2000.

J. Wahlström and L. Eriksson. Robust nonlinear egr and vgt control with integral action for diesel engines. In *Proc. 17th IFAC World Cong.*, pages 2057–2062, 2008.

J. Wahlström and L. Eriksson. Nonlinear egr and vgt control with integral action for diesel engines. *Oil & gas science and technology*, 66:573–586, 2011a.

J. Wahlström and L. Eriksson. Modelling diesel engines with a variable-geometry turbocharger and exhaust gas recirculation by optimization of model parameters for capturing non-linear system dynamics. *J. of Automobile Engineering*, 225:960–986, 2011b.

J. Wahlström, L. Eriksson, and L. Nielsen. Egr-vgt control and tuning for pumping work minimization and emission control. *IEEE Trans. Control Systems Technology*, 18: 993 –1003, 2010.

Q. Zhang and A. Benveniste. Wavelet networks. *IEEE Transactions on Neural Networks*, 3:889–898, 1992.

Appendix A. NOMENCLATURE

Table A.1. List of variables

General	$\dot{m}$	Mass flow
	ω	Rotational speed
	COV	Change-Over-Valve
	O	Oxygen concentration
	p	Pressure
	T	Temperature
	VGT	Variable-Geometry-Turbocharger
$\boldsymbol{u}, \boldsymbol{d}, y$	ω_{blow}	Rotational speed of blower
	u_{egr}	Opening signal for COV
	u_{load}	Engine load
	u_{vgt}	Opening signal for VGT
	O_{scav}	Scavenge oxygen concentration
States	p_{scav}	Scavenge manifold pressure
	p_{exh}	Exhaust manifold pressure
	p_{blow}	Pressure in the EGR plenum
	O_{scav}	Scavenge oxygen concentration
	O_{exh}	Exhaust oxygen concentration
	ω_t	Turbocharger rotational speed
	$\tilde{u}_{vgt}$	Dynamics of u_{vgt}
	$T_{1,k}$	Internal engine temperature
	$x_{r,k}$	Gas fraction in engine